



Bowl-in-bowl complex formation with mixed sized calixarenes: Adaptivity towards guest binding

Journal:	<i>ChemComm</i>
Manuscript ID	CC-COM-04-2018-003415.R1
Article Type:	Communication

SCHOLARONE™
Manuscripts



Journal Name

COMMUNICATION

Bowl-in-bowl complex formation with mixed sized calixarenes: Adaptivity towards guest binding

Arnab Dawn,^a Andrew Eisenhart,^b Marzieh Mirzamani,^a Thomas L. Beck,^{b*} and Harshita Kumari^{*a}

Received 00th January 20xx,
Accepted 00th January 20xx

DOI: 10.1039/x0xx00000x

www.rsc.org/

We demonstrated the organization of two differently sized calixarenes C-methylresorcin[4]arene (RsC1) and either Calix[6]arene (Calix6) or Calix[8]arene (Calix8), where the lower rim of RsC1 partially overlaps with the upper rim of Calix6 or Calix8. An adaptive nature of the heteromacrocyclic assembly towards binding of a model guest has been observed.

Synthetic nanocarriers mimicking *in vivo* biological vehicle such as exosomes, are at the focal point of nanomedicine research powering therapeutic control.¹ In this global surge of miniaturizing tools and technologies for customized applications, engineered cavities with defined size, shape, and selectivity, could potentially resolve the dual issue of immobilization and targeted delivery.² In this paper, we have focused our efforts on engineering a completely new class of supramolecular cavity containing architectures, with the help of differently sized calixarenes arranged in a 'bowl-in-bowl' fashion. Based on feasibility studies with the theoretical calculations, the experimental analysis indicated the formation of such a heteromacrocyclic assembly for the first time.

Controlling cavity geometries in spaces is a challenge in supramolecular chemistry, which limits applications in synthetic biomimetics. Common examples of such cavitands includes cyclodextrins,³ calixarenes and analogues,⁴ pillarenes,⁵ and cucurbiturils.⁶ These cavitands primarily differ in symmetry, shape and hydrophilicity. For example, cyclodextrins and calixarenes primarily adopt a cone architecture with non-identical cavity gates (upper and lower rims). Pillarenes and cucurbiturils, on the other hand, are symmetric with identical cavity gates. Aqueous solubility and biocompatibility makes cyclodextrin popular in pharmaceutical sectors,⁷ whereas ease of synthesis and functionalization, make calixarenes one of the

most investigated macrocycles for the last five decades. The guest binding property of calixarenes and their sister derivatives, resorcinarenes and pyrogalloarene crucially relies on the macrocycle conformation. Among all, a crown or the bowl-shaped conformation is considered to be the most effective for guest binding, because of the defined cavity size and shape. However, the flexibility of the conformations increases with increase in ring sizes. This is why calixarenes with a ring size of four is the most exploited species in this group.

Apart from the individual macrocycles, self-assembled macrocycles forming discrete geometries offer extended cavity features based on the ring size, solvent, ligand, guest and/or metal salts.⁸ Calixarene based supramolecular polymers also provide a wide range of extended macrocyclic arrays bridged by various types of noncovalent linkers.⁹ However, in both cases, linkers or guest molecules occupy the macrocycle cavity partially or completely. On the other hand, covalently coupled systems with defined cavity features require complex synthetic methods.¹⁰ A supramolecular alignment of macrocycles in space without the help of a linker is non-existent in the literature. There is only one report of crystallization of a smaller cucurbituril sitting inside a larger cucurbituril.¹¹

To overcome the issue, we hypothesized that two primary criteria need to be satisfied. Firstly, the two macrocycles should interact with each other in a specific direction, and secondly, the overlap between two units needs to be partial in nature to utilize the extended cavity feature. Two similar types of macrocycles with different ring sizes could fulfil the first criterion because of similar surface curvature and size compatibility (smaller with larger). On the other hand, a crown (bowl-shaped) conformation could be an ideal candidate preventing a complete inclusion because of the differently sized cavity gates at either of the ends. Thus, only bowl-shaped heteromacrocyclic assemblies can satisfy the above criteria.

In our approach, we have programmed two macrocyclic host molecules complemented in size and shape, offering a series of potential pre-organized host assemblies based on kinetic and thermodynamic preferences. We have selected

^a College of Pharmacy, University of Cincinnati, Cincinnati OH 45267-0004, USA
E-mail: kumariha@ucmail.uc.edu

^b Department of Chemistry, University of Cincinnati, Ohio 45221, USA

^c Email: becktl@ucmail.uc.edu

Electronic Supplementary Information (ESI) available: [details of any supplementary information available should be included here]. See DOI: 10.1039/x0xx00000x

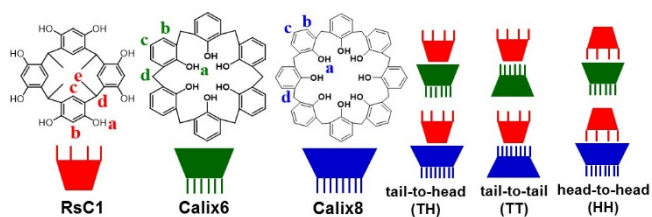


Fig. 1 Molecular structures of the macrocycles used, and illustration of possible modes of arrangement between RsC1 with either Calix6 or Calix8.

C-methylresorcin[4]arene (RsC1) as the smaller bowl, and either calix[6]arene (Calix6) or calix[8]resosrcinarene (Calix8) as the larger bowls, based on their structural simplicity and easy availability (synthetically or commercially). We preferred RsC1 over the Calix[4]arene as the smaller bowl, to minimize the steric and electronic repulsion of hydroxyl groups with the larger bowl (Fig. 1). The upper and lower rim of the macrocycles are designated as ‘head’ (H) and ‘tail’ (T), respectively. Also, in naming a particular organization mode, the smaller bowl (RsC1) precedes the larger bowl (Calix6 or Calix8). We ruled out the HT mode of interaction because of the similar face sizes, and steric hindrance among the hydroxyl groups.

First, we predicted the feasibility of aligning the macrocycles in a bowl-in-bowl fashion, using free energy calculations. The systems consisted of 1800 molecules of methanol and DMSO, and two macrocycles (RsC1 with either Calix6, or Calix8) in an approximately 7 nm cube simulation cell with the two macrocycles placed 3 nm apart along the z-axis. Macrocycle conformations were based upon geometry optimizations done using the Gaussian09 suite of programs, using the B3LYP functional and 6-31G** basis set. The CHARMM general force field was chosen to model the macrocycles and DMSO with parameters assigned by analogy using the Cgenff utility.¹² Parameters used to describe the methanol molecules were used previously by Spoel et al.¹³ All MD simulations were carried out using the GROMACS code and suite of utilities.¹⁴ A time step of 2 fs was used for all calculations. Long range electrostatics were represented using the PME algorithm. The Nose-Hoover¹⁵ thermostat and the Parrinello-Rahman barostat¹⁶ were used to regulate the temperature and to reach the appropriate density. All potentials of mean force (PMFs) were computed using the combined weighted histogram analysis method¹⁷ (WHAM) and umbrella sampling available in GROMACS. The PMFs were calculated along the z-axis, which corresponds to the separation distance (r) between the two macrocycles center of mass. Tests of reversibility and pulling speed’s effect also reinforce that convergence has been reached.¹⁸ Calix[4]arene’s relaxation time is 150ps in water.¹⁹ Thus each umbrella sampling window is simulated 40 times longer to allow for complete relaxation. The accuracy of the PMFs was assessed via Bootstrap analysis, also present in the GROMACS WHAM module. Each PMF was treated with 200 bootstrap iterations with each histogram generated previously used as independent data points. Using this method, the average profile and standard deviation of each run is generated. The hypothesized interaction between RsC1 and Calix6 in the TH orientation produces the PMF curve as shown in Fig 2. This PMF implies that the minimum for the interaction is reached when the centers of mass are 0.57 nm

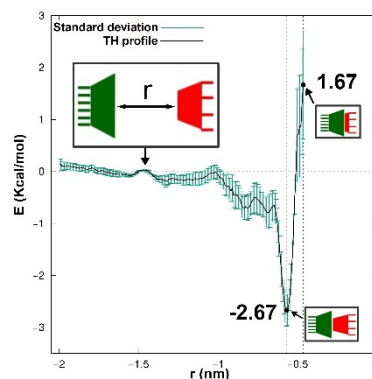


Fig. 2 Hypothesized interactions between RsC1 and Calix6 in TH orientation.

apart. Comparison with the hypothesized interactions involving HH and TT configurations clearly shows the preference for the TH configuration (Fig S1, ESI). The HH and TT configurations both have not only smaller magnitude minima, but the minima are also located at a larger COM distance. All PMFs have been zeroed at 2.6 nm for ease of comparison. Next, we have performed a similar study by replacing Calix6 with Calix8 (Fig S2, ESI). For ease of comparison, both PMFs have been zeroed to 1.5 nm. When compared to the PMFs for the RsC1 and Calix6 macrocycle interactions it can be seen that the minima are located at similar distances (0.62 nm), however, these minima are smaller in magnitude. Thus from the theoretical analysis it is evident that the TH mode of interactions between RsC1 and calix6 or calix8 is energetically feasible.

Stirring equimolar RsC1 with Calix6 or Calix8 separately at room temperature (RT) in DMSO- d_6 did not show any significant change as studied by ^1H NMR (Fig S3, ESI). This implies that under such a condition interaction between two differently sized macrocycles is not favorable. However, the theoretical analysis prompted us to consider that perhaps a higher energy barrier, compared to what theoretical analysis predicts, might have been involved. We envisioned that an external source of energy (such as thermal energy) might help to cross such an energy barrier. Thus, we exposed the same reaction mixtures at 393 K for 1 h, and the color turned darker. This time NMR results show noticeable changes in RsC1-Calix6 and RsC1-Calix8 spectra (Fig S4, ESI). Signals associated with hydroxyl and aromatic protons of RsC1 (marked as a, b and c in Fig 1) experience severe broadening in both the systems. This is associated with a restricted motion in the presence of another macrocycle. Other changes of RsC1 protons are the bridging proton ‘d’ and the methyl proton ‘e’. On the other hand, the broadening associated with Calix6 or Calix8 aromatic protons (b and c) are less but still demonstrates an interaction. Interestingly, the extent of broadening is more in the case of the RsC1-Calix8 system. Thus, it appears at this point that increasing the size of the larger bowl might enhance the interaction with the smaller bowl. We rule out the possibility of conformational rearrangement at a high temperature, based on a control experiment where RsC1 (most affected bowl among the three) ^1H NMR shows only a minor broadening upon heating in DMSO- d_6 at 393 K for 1 h (Fig S5, ESI). Although the theoretical analysis predicted the TH mode of interaction as the most favored, the

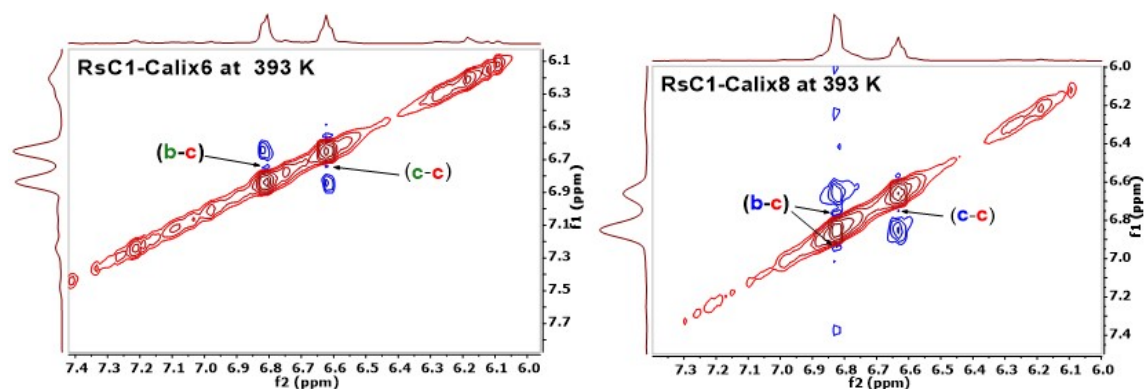


Fig. 3. ROESY NMR spectra of RsC1-Calix6 and RSC1-Calix8 in DMSO- d_6 , prepared at 393 K (correlation between protons from different macrocycles are indicated)

1D NMR alone was unable to justify the same. Therefore, we performed the ROESY NMR of the reaction mixtures obtained at 393 K. Interestingly, we observed clear correlations among aromatic protons of RsC1 and either Calix6 or Calix8 (Fig 3, and Fig S6, ESI). It is worth noticing that between two different aromatic protons in RsC1 (b, c), only 'c' shows a correlation with the aromatic protons (b, c) of Calix6 or Calix8. This clearly indicates that the lower rim of the smaller bowl RsC1 partially overlaps with the upper rim of the larger bowls Calix6 or Calix8. This is nothing but a TH mode of interaction between two differently sized bowls, as predicted by the theoretical analysis. It can also be noticed from ROESY NMR that the interaction of proton 'c' of RC1 is stronger with the proton 'b' compared to the proton 'c' of the larger bowls in either Calix6 or Calix8. This is reasonable because the number of aromatic units are different in a smaller bowl and a larger bowl, and therefore a face-to-face aromatic stacking is not expected. To the best of our knowledge, this is the first report in which aligning of two macrocycles linearly in supramolecular fashion is observed. We term this a 'bowl-in-bowl' formation as an illustrative way of describing the configuration. The synthesized heteromacrocyclic assemblies at high temperature were found to be stable over time as evident from practically unaltered NMR spectra (Fig S7, ESI). This signifies the robustness of the complex with aging, and over a temperature range.²⁰

Further, we have performed small angle neutron scattering (SANS) which is a powerful tool for unveiling the solution phase assembly structure.²¹ SANS measurements for RsC1-Calix6 and RsC1-Calix8 were taken at NGB 30 m SANS instrument at the NIST Center for Neutron Research (NCNR) in Gaithersburg, MD, USA. The collected SANS data ($0.0034 \text{ \AA}^{-1} < q < 0.41 \text{ \AA}^{-1}$) was reduced and fitted to variety of models (Sphere, Ellipsoid, Cylinder, and Bimodal Schulz Sphere) which was summed to the power law model to account for the increased low-Q scattering. Among the different form factor models we tested, the sphere model was the best model fit (Fig 4 and Table S2, ESI). The SANS fitting results show that upon heating (393 K) the radius of RsC1-Calix6 nanoassembly decreases from 6.5 \AA to 5.9 \AA . This is in agreement with the NMR results, displaying a closer approach of RsC1 and Calix6 at an elevated temperature, thus favoring interactions between the macrocycles. In contrast, the radius of RsC1-Calix8 nanoassembly ($R \sim 7.5 \text{ \AA}$) remains practically

unchanged. This can be attributed to (a) the conformational flexibility of Calix8 due to its large ring size; (b) presence of two energy minima (Fig S8) suggesting RsC1 and Calix8 can interact at two distances. The increase in overall particle size for RsC1-Calix8 compared to RsC1-Calix6 is because of the larger size of Calix8 compared to Calix6.

Based on the experimental results, we extended our theoretical analysis, and the change in PMF for TH the most preferred configuration, was tested at an elevated temperature. The PMFs of RsC1-Calix6 at 400K show an enhanced minima and is still located in the same area (Fig S8a, ESI). The simulations done with RsC1-Calix8 at 400K (Fig S8b, ESI) conversely show a minimum of reduced depth and an interaction further away. There are still two minima perhaps indicating a shared solvent minimum and ring contact minimum.

Finally, we have tested the usefulness of our bowl-in-bowl systems over the single bowls, by binding with a model guest 4-aminobiphenyl (AMB) which is known as human bladder carcinogens and widely used in case studies to investigate the cancer.²² While the presence of phenyl ring would facilitate the guest inclusion, presence of two rings offers the unique opportunity of differentiation between single bowls and bowl-in-bowl in terms of cavity environment and guest fitting. We studied the host-guest binding by ^1H NMR in DMSO- d_6 /D $_2$ O (4:1, v/v) to facilitate the guest binding driven by hydrophobic force, and also to test the water compatibility which is a vital issue for applying such a system in presence of biologically relevant molecules.²³ It is worth noticing that a significant downfield shift of the aromatic protons of ABP could be observed in presence of RsC1-Calix6 and RsC1-Calix8 (Fig S9, ESI).²⁴ Such an effect is much less pronounced in case of the single bowls, RsC1, Calix6, and Calix8. Interestingly, in presence of RsC1-Calix6, ABP aromatic proton signal splits, which can be attributed to the anisotropic microenvironment the guest experiences because of restricted rotational freedom inside the host cavity.²⁵ This supports that the bowl-in-bowl systems indeed offer an extended cavity to accommodate larger guest, and at the same time supramolecular nature of binding between two bowls induces self-additivity in the host in fine-tuning the cavity feature for most efficient guest binding (Fig S10, ESI).²⁶

In this study, we have used simple molecular systems.

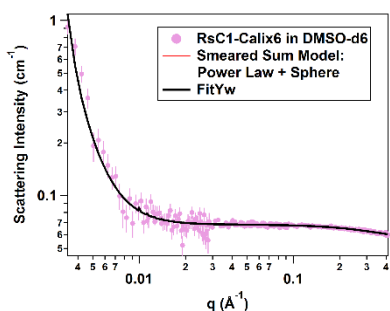


Fig. 4 Example fit of a smeared Power Law+Sphere model to RsC1-Calix6 SANS data.

Further functionalization of the hosts for additional interaction sites, and various combinations of hosts, can create a library of organizing cavity-containing systems towards developing more complex geometries.

In conclusion, we synthesized two bowl-in-bowl ensembles of resorcinarene (smaller macrocycle), with either calix[6]arene or calix[8]arene (larger macrocycles). Theoretical analysis predicted the feasibility of such a process at room temperature. However, only the high temperature experiments shows similar findings, as evidenced by NMR and SANS studies. Interaction between the lower rim of the resorcinarene with the upper rim of either calix[6]arene or calix[8]arene in bowl-in-bowl fashion, is found to be the most favorable among all possible alignments. The bowl-in-bowl complex containing calix[6]arene demonstrates an adaptive binding behavior towards a model guest. The present approach can revolutionize the synthesis of complex adaptive cavity geometries by using simple supramolecular building blocks, and their potential usage in transport and delivery applications.

The work is supported by the startup funds CoP, UC (H.K.). We acknowledge NSF grant CHE-1565632 for partial support (TLB). We also acknowledge an extensive grant of computer resources at the Ohio Supercomputer Center where the simulations were performed. We thank Dr. Boulem Hammouda for the help in SANS experiment set up at NIST.

Conflicts of interest

Authors declare no conflicts of interest

Notes and references

- a) L. Alvarez-Erviti, Y. Seow, H. F. Yin, C. Betts, S. Lakhali and M. J. A. Wood, *Nat. Biotechnol.*, 2011, **29**, 341; b) E. Fleige, M. A. Qadir and R. Haag, *Adv. Drug Deliv. Rev.*, 2012, **64**, 866.
- a) A. C. Steven, W. Baumeister, L. N. Johnson and R. N. Perham, *Molecular Biology of Assemblies and Machines*, Garland Science, 2016; b) B. J. G. E. Pieters, M. B. van Eldijk, R. J. M. Nolte and J. Mecnovic, *Chem. Soc. Rev.*, 2016, **45**, 24.
- a) E. Engeldinger, D. Armspach and D. Matt, *Chem. Rev.*, 2003, **103**, 4147; b) L. Peng, S. Liu, A. Feng and J. Yuan, *Mol. Pharmaceutics*, 2017, **14**, 2475; c) N. Sharma and A. Baldi, *Drug Deliv.*, 2016, **23**, 729.
- a) C. D. Gutsche and L. J. Bauer, *J. Am. Chem. Soc.*, 1985, **107**, 6052; b) K. Kobayashi and M. Yamanaka, *Chem. Soc. Rev.*, 2015, **44**, 449; c) W. Sliwa, *J. Incl. Phenom. Macrocycl. Chem.*, 2005, **52**, 13; d) C. Wieser, C. B. Dieleman and D. Matt, *Coord. Chem. Rev.*, 1997, **165**, 93.
- a) T. Ogoshi, *J. Incl. Phenom. Macrocycl. Chem.*, 2012, **72**, 247; b) L-L. Tan and Y-W. Yang, *J. Incl. Phenom. Macrocycl. Chem.*, 2015, **81**, 13.
- a) S. J. Barrow, S. Kasera, M. J. Rowland, J. del Barrio and O. A. Scherman, *Chem. Rev.*, 2015, **115**, 12320; b) E. Masson, X. Ling, R. Joseph, L. Kyeremeh-Mensah and X. Lu, *RSC Adv.*, 2012, **2**, 1213; c) J. W. Lee, S. Samal, N. Selvapalam, H-J. Kim and K. Kim, *Acc. Chem. Res.*, 2003, **36**, 621; d) L. Isaacs, *Acc. Chem. Res.*, 2014, **47**, 2052.
- a) S. V. Kurkov and T. Loftsson, *Int. J. Pharm.*, 2013, **453**, 167; b) M. Pio di Cagno, *Molecules*, 2017, **22**, 1; c) L. Leclercq, *Beilstein J. Org. Chem.* 2016, **12**, 2644.
- a) H. Kumari, A. V. Mossine, S. R. Kline, C. L. Dennis, D. A. Fowler, S. J. Teat, C. L. Barnes, C. A. Deakyne and J. L. Atwood, *Angew. Chem. Int. Ed.*, 2012, **51**, 1452; b) K. D. Shimizu and J. Rebek, Jr. *Proc. Natl. Acad. Sci.*, 1995, 12403; c) H. Kumari, C. A. Deakyne and J. L. Atwood, *Acc. Chem. Res.*, 2014, **47**, 3080; d) P. P. Cholewa and S. J. Dalgarno, *Cryst. Eng. Comm.*, 2014, **16**, 3655; e) C. M. Mayhan, A. M. Drachnik, A. V. Mossine, H. Kumari, D. A. Fowler, C. L. Barnes, S. J. Teat, J. E. Adams, J. L. Atwood and C. A. Deakyne, *J. Phys. Chem. C*, 2016, **120**, 13159.
- D-S. Guo and Y. Liu, *Chem. Soc. Rev.*, 2012, **41**, 5907.
- a) R. Pinalli, M. Suman and E. Dalcanale, *Eur. J. Org. Chem.*, 2004, 451; b) R. J. Hooley and J. Rebek, Jr. *Chem. Biol.*, 2009, **16**, 255. c) D. M. Rudkevich and J. Rebek, Jr. *Eur. J. Org. Chem.*, 1999, 1991; d) T. Chavagnan, D. Semeril, D. Matt and L. Toupet, *Eur. J. Org. Chem.*, 2017, 313; e) J. Murray, K. Kim, T. Ogoshi, W. Yao and B. C. Gibb, *Chem. Soc. Rev.*, 2017, **46**, 2479.
- A. I. Day, R. J. Blanch, A. P. Arnold, S. Lorenzo, G. R. Lewis and I. Dance, *Angew. Chem. Int. Ed.*, 2002, **41**, 275.
- K. Vanommeslaeghe and A. D. MacKerell, Jr. *J. Chem. Inf. Model*, 2012, **52**, 3144.
- N. M. Fischer, P. J. van Maaren, J. C. Ditz, A. Yildirim and D. van der Spoel, *J. Chem. Theory Comput.*, 2015, **11**, 2938.
- M. J. Abraham, T. Murtola, R. Schulz, S. P'all, J. C. Smith, B. Hessa and E. Lindahl, *SoftwareX*, 2015, **1-2**, 19.
- D. J. Evans and B. L. Holian, *J. Chem. Phys.* 1985, **83**, 4069.
- M. Parrinello and A. Rahman, *J. Appl. Phys.* 1981, **52**, 7182.
- J. S. Hub, B. L. de Groot and D. van der Spoel, *J. Chem. Theory Comput.*, 2010, **6**, 3713.
- C. D. Christ, A. E. Mark and W. F. van Gunsteren, *J. Comput. Chem.*, 2010, **31**, 1569.
- F. M Ytreberg, *J. Phys. Chem. B*, 2010, **114**, 5431.
- G. H. Aryal, K. I. Assaf, K. W. Hunter, W. M. Nau and L. Huang, *Chem. Commun.* 2017, **53**, 9242.
- a) H. Kumari, S. R. Kline, N. J. Schuster, C. L. Barnes and J. L. Atwood, *J. Am. Chem. Soc.*, 2011, **133**, 18102; b) H. Kumari, S. R. Kline, C. L. Dennis, A. V. Mossine, R. L. Paul, C. A. Deakyne and J. L. Atwood, *Angew. Chem. Int. Ed.*, 2012, **51**, 9263; c) H. Kumari, S. R. Kline, D. A. Fowler, A. V. Mossine, C. A. Deakyne and J. L. Atwood, *Chem. Commun.*, 2014, **50**, 109.
- a) T. Yagi, Y. Fujikawa, T. Sawai, T. Takamura-Enya, S. Ito-Harashima and M. Kawanishi, *Toxicol. Res.*, 2017, **33**, 265; b) S. M. Cohen, A. R. Boobis, M. E. Meek, R. J. Preston and D. B. McGregor, *Crit. Rev. Toxicol.*, 2006, **36**, 803.
- G. H. Aryal, C. H. Battle, T. A. Grusenmeyer, M. Zhu and J. Jayawickramarajah, *Chem. Commun.*, 2016, **52**, 2307.
- The reason for deshielding is probably the result of the complicated nature of aromatic ring current arises from the close proximity of molecularly (in ABP) and supramolecularly (in bowl-in-bowl complex) bound multiple aromatic systems.
- W-H. Chen, M. Fukudome, D-Q. Yuan, T. Fujioka, K. Mihashi, and K. Fujita, *Chem. Commun.*, 2000, 541.
- Guest binding and guest release as the functions of guest size, shape, and functionality, are under investigations.